Title
PHOTOMULTIPLIER SINGLE-ELECTRON STATISTICS

Authors
Tusting, Robert F.
Kerns, Quentin A.
Knudsen, Harold K.

Publication Date
1962-02-21

University of California

Ernest O. Lawrence Radiation Laboratory

Berkeley, California

DISCLAIMER

UCRL-9980
Limited Distribution

UNIVERSITY OF CALIFORNIA

Lawrence Radiation Laboratory
Berkeley, California

Contract No. W-7405-eng-48

PHOTOMULTIPLIER SINGLE-ELECTRON STATISTICS

Robert F. Tusting, Quentin A. Kerns, and Harold K. Knudsen

February 21, 1962

PHOTOMULTIPLIER SINGLE-ELECTRON STATISTICS*

Robert F. Tusting, Quentin A. Kerns, and Harold K. Knudsen

Lawrence Radiation Laboratory
University of California
Berkeley, California

Summary

Our measurements of the amplitude distribution of photomultiplier anode pulses due to the emission of single-electrons from the cathode consistently show a peak. It is significant that the peak position agrees with that of a calculated distribution based on a Poisson distribution of secondary electrons at each dynode. The integral distribution, obtained by counting single-electron pulses, tends to show a plateau.

In low-light-level counting applications, one can set the discriminator so that a majority of photomultiplier single-electron pulses will be counted. Further increase in the sensitivity will eventually increase the noise rate faster than the counting efficiency.

The techniques for measuring photomultiplier single-electron statistics are useful for obtaining comparative collection efficiencies. By single-electron measurements, one can adjust focusing-electrode potentials to maximize overall collection efficiency.

It is believed that there is some correlation between the amplitude and time distributions. Further work is necessary to show the extent of the correlation.

Introduction

The response of photomultipliers to single photoelectron inputs has been studied for several reasons:

(a) It is important to the understanding of the basic (and not thoroughly understood) processes of secondary emission.

(b) The response to single electrons is helpful in predicting the response to arbitrary pulses.

(c) Single-electron response measurements are an aid in the selection and comparison of photomultipliers and methods of operating them in critical applications.

A system for making such measurements must be capable of causing the cathode to emit a single electron, and recording the amplitude and time delay of the resulting anode pulse. The system must also be capable of separating the signal pulse from the background noise of the multiplier.

Light Source Considerations to Secure Single Photoelectrons

A mercury-capsule light-pulse generator provides brief, accurately timed, light flashes.[1,2] In order to secure light flashes of the shortest duration, the high voltage is kept below 1 kv. When the light is seen through a 4400Å filter, (such as Corning No. 5113)intensity vs time is a curve that rises rapidly to a peak, decays somewhat more slowly nearly to zero, and continues decreasing on a still longer low-intensity tail. The duration between the 50% intensity points is less than 1 nsec, and at low voltages, 80% of the total photon output is emitted within 2 nsec. The light source is used to generate single photoelectron signals in the following manner.

The mean number of photons observed per light flash may be large--e.g. 10^4. If one now places optical attenuation of 10^5X between the light source and the observer,† the previous curve of light intensity vs time is interpreted as the relative probability as a function of time of seeing photons, and the mean number of photons per flash is now 1/10. If these photons strike a photocathode of 20% quantum efficiency, the mean number of photoelectrons per flash is 1/50. The optical attenuator and the photocathode perform an independent random selection of those photons that are to pass the attenuator and eject a photoelectron. For these small numbers, a good approximation is the Poisson formula,

$$P_r = \frac{\epsilon^r}{r!} e^{-\epsilon} ,$$

where ϵ is the expected number of photoelectrons per flash, and P_r is the probability of obtaining exactly r photoelectrons in a single flash. We observe that

$$\frac{P_{r+1}}{P_r} = \frac{\epsilon}{r+1} .$$

In the present example, we have $\epsilon = 1/50$; thus the probabilities of obtaining zero, one, two, three----r electrons are, respectively:

$$P_0 = \frac{\epsilon^0}{0!} e^{-1/50} \approx 0.98,$$

$$P_1 = \epsilon P_0 \approx 0.0196,$$

$$P_2 = \frac{\epsilon P_1}{2} = \frac{P_1}{100},$$

$$P_3 = \frac{\epsilon P_2}{3} = \frac{P_1}{15,000} ,$$

*This work was done under the auspices of the U. S. Atomic Energy Commission.

† Kodak neutral-density Wratten filters (No. 96) are convenient for this purpose.

$$P_r = \frac{\epsilon P_{r+1}}{r} .$$

In this example, most nonzero pulses will be single electrons, with a small contamination (~1%) of multiple-electron pulses. Typically, we set $1/10 \geq \epsilon \geq 1/100$; thus the light must be flashed on the average 10 to 100 times to secure a single nonzero pulse. The value of ϵ is not critical, providing it is small, and some fluctuation of ϵ is permissible.

System Block Diagram

Figure 1 illustrates the system used for the measurements. The light flasher is continously driven mechanically at 60 pulses/sec but emits light only when the high-voltage gate is on. The number of phototube output pulses is registered on the photomultiplier-output-pulse counter. The number of light flashes is registered on the light pulse counter. The ratio of the two counter totals is approximately ϵ, providing that most of the photoelectrons leaving the cathode enter the multiplier and result in a detectible output pulse.

The cycle of operations is as follows: A start pulse resets the charge-amplitude counter and gates on the light-flasher high voltage. The light then flashes at the rate of 60/sec until a photomultiplier output pulse occurs, at which time the high voltage is gated off until the charge amplitude can be read out.

To reduce the smearing of data by phototube noise pulses, a time coincidence is required between a phototube output pulse and a suitably delayed trigger pulse from the light flasher. Thus the accidental noise rate is reduced by the duty factor of the signal gate. Since the gate is opened after every light flash, the ratio of noise to signal pulses increases as ϵ decreases, which imposes a practical lower limit on ϵ.

Charge-Amplitude Measurements

If an electron enters the multiplier, one expects an amplified pulse of charge to be collected at the anode somewhat later. The result of measuring and recording the anode charge for each of many pulses is the distribution of the output-pulse amplitudes for single-electron input signals. In Fig. 1, pulses at A and B provide information for obtaining the delay time between the light flash and the output pulse.

Experience with feedthrough and nonlinearity problems in available linear gates dictates that the height analysis precede the coincidence. A lumped LCR circuit directly connected to the phototube anode proved successful in measuring the anode charge amplitude (see Fig. 2.) Two modes of operation are possible by changing the damping. In the first, the damping is moderate (R is entirely due to the reflected amplifier input resistance), and the arriving charge ballistically excites a decaying 10-Mc cosine wave. The waveform is linearly amplified and presented to an amplitude discriminator. A train of pulses emerges from the discriminator, one pulse for each loop of the sinusoid above the discriminator threshold. Thus the number of output pulses is proportional to the logarithm of the phototube charge amplitude. This number appears on the charge-amplitude counter. The necessary dynamic range of 100:1 is achieved easily in 20 channels. Owing to the gate length required (~ 2 μsec), low-noise tubes must be selected for this case.

The second mode of operation involves critical damping of the LCR circuit to produce a single zero-crossing pulse,[3] which trips the discriminator only once on the backswing of the pulse. The discriminator threshold level is changed stepwise to build up the integral pulse-height distribution. The charge-amplitude counter is reset only once at each threshold level change. In this mode, the gate width can be reduced to approximately the time spread of the tube, allowing measurements on relatively noisy tubes.

Charge Calibration

For charge-calibration purposes (see Fig. 2), a small three-terminal capacitor (0.160 pf) is permanently connected between the end of a terminated cable and the phototube anode.* The step-function generator feeds voltage pulses of known amplitude, V, via the cable to the 0.16-pf capacitor. Since the total capacitance at the phototube anode is approximately 15 pf, the test charge delivered to the anode circuit from the step generator is very nearly

$$q = 0.16 \times 10^{-12} \times V$$

or, since $e = 1.602 \times 10^{-19}$ coulomb,

$$q = 10^{6} \text{ electrons/volt.}$$

The rise of the step-function generator pulse is adjusted to match the shape of the test charge with that of the photomultiplier pulse.

Using the charge calibration circuit, one can conveniently deposit an accurately known test charge of from 10^4 to 10^8 electrons on the anode.

Statistics of Electron Multiplication

Various reference to this subject can be found in the literature. Van der Ziel remarks that, on the basis of noise measurements, the probability

---

*We constructed a three-terminal capacitor by in effect making a 1 in. length of Teflon-insulated 100-ohm coax line, and cutting the center conductor in two to leave a gap. The capacitance value was adjusted to 0.16 pf ± .1% on a transformer-ratio capacitance bridge. For ease of capacitance setting, one of the center conductors was threaded.

distribution of secondary electrons may be Poisson for low primary energies (< 150 v).[4] J. A. Baicker found a simple exponential pulse-height distribution for pulses due to single electrons.[5]

Lombard and Martin have calculated the pulse-height distribution at the anode of an electron-multiplier structure due to single-electron inputs with a Poisson distribution assumed at each stage.[6] In their calculations, they assumed equal interstage gain, m, choosing values for m of 1.5, 2.0, 3.0 and 5.0. Their results indicated that a definite peak should be observed if the electron multiplication obeys Poisson statistics, but in their experimental work, no peak was observed. They suggest that Poisson statistics do not give the correct distribution.

Figure 3 is taken from Lombard and Martin,[6] and shows their calculation (which they do not find experimentally). Figure 4 is an integral pulse-height distribution obtained by integration of the Lombard and Martin curves, and thus shows calculated relative counting rates as a function of the discriminator threshold for the various values of interstage multiplication, m.

Photomultiplier measurements made with the system of Fig. 1 consistently show a peak in the distribution. Figure 5 shows the peak clearly. For $3 < m < 5$, there is a rough fit with the Lombard and Martin curves. As a compact description of the approximate form of the pulse-height distribution, we have used the simple function $x^{\alpha} e^{-\beta x}$. This function, with $\alpha = \beta = 1$, is presented in Fig. 5.

The integral counting-rate curves tend to show a plateau with increasing discriminator sensitivity, since there are relatively few of the very small pulses. Examples are given in Fig. 6. In a counting experiment involving low light levels, one should provide sufficient gain to reach the plateau, but little counting efficiency is gained by going further, whereas the interfering effects of noise continue to rise with increasing gain.

- -

In the following discussion the effects of noise are excluded. A single electron leaving the photocathode will result in an output pulse of x electrons collected by the anode, for $0 \lesssim x < \infty$. Events with $x = 0$ may conveniently be regarded as separate from those with $x > 0$.

If λ is the probability that an $x > 0$ event happen, $1 - \lambda = P_0$ is the probability than an $x = 0$ event happen, and $P(x)$ is the amplitude distribution of the $x > 0$ events, the normalization condition is

$$\int_0^{\infty} P(x)dx = \lambda .$$

There are a number of reasons for λ being less than unity, e.g., imperfect electron optics and finite secondary-emission gain.

It is convenient to think of λ as an overall collection efficiency, and $\bar{x}$, the mean of the $P(x)$ distribution, as a single-electron pulse gain. We can relate the dc gain to λ:

$$\text{dc gain} = \frac{\text{anode current}}{\text{cathode current}} = \lambda\bar{x} ,$$

and hence

$$\lambda = \frac{\text{dc gain}}{\bar{x}} .$$

To maximize λ, one must usually degauss and magnetically shield the tube, as well as carefully adjust the various focusing-electrode potentials.

Collection Efficiency

Figures 7 and 8 were obtained by pulsed illumination of successive areas of the phototube. The plateau counting rate was measured for each chosen area. This rate is proportional to the product of quantum efficiency, illuminated area, and overall collection efficiency; thus knowing the quantum efficiency, one can obtain the relative collection efficiency. The points shown represent the count obtained after subtracting noise pulses.

Noise Considerations

Noise arises both in the phototube and in following circuits. The phototube delivers noise pulses that are in part due to amplified thermionic emission at the cathode (see reference 5 for additional information). The circuit noise on the other hand is primarily thermal and shot noise. One can examine the circuit noise alone by removing the phototube and inserting an equal "dummy" capacitance. In this fashion, the integral pulse-height spectrum has been measured for the total circuit noise in terms of a counting rate vs the discriminator charge threshold. If we fit the measured points to a 1-erf(x) curve, on the assumption that the charge fluctuates in a Gaussian fashion about a mean of zero, the noise counting rate in pulses per minute is

$$\text{noise counting rate} \approx 4.9 \times 10^8 [1 - \text{erf}(\alpha)],$$

where

$$\alpha = \frac{\text{discriminator threshold (number of electrons)}}{7{,}400}$$

and

$$\text{erf}(x) = \frac{2}{\sqrt{\pi}} \int_0^x e^{-x^2} dx .$$

This suggests that there is a root-mean-square (rms) noise charge of 5,200 electrons. However, from thermal-noise consideration, one expects a fluctuating charge at the phototube-anode circuit such that the mean energy in the capacitance (15 pf total) equals kT/2, i.e.,

$$\frac{C\overline{V^2}}{2} = \frac{\overline{q^2}}{2C} = \frac{1}{2} kT ,$$

or

$$\sqrt{\overline{q^2}} = \sqrt{CkT} = (15\times10^{-12}\times1.38\times10^{-23}\times300)^{1/2}$$

$$= 2.5\times10^{-16} \text{ coulombs}$$

$$= 1,600 \text{ electrons.}$$

Since the apparent measured rms charge is about three times the calculated value, the amplifiers are clearly not ideal, but it is evident that to make a substantial improvement would require low temperatures or parametric techniques. With the present amplifiers, which have a noise factor of ~ 10 db, the discriminator threshold must be several times the 7,400 electron level to keep the circuit noise rate small.

The discriminator threshold was set above a 40,000 electron level for all pulse distribution measurements ($\alpha > 5$), and circuit noise was not a significant factor. The photomultipliers were operated at a dc gain $\geq 1.3\times10^6$ (see Table I).

Time Distributions

Zero-crossing tunnel-diode circuits represent good technique for timing the single electron pulses.[3] Since amplitude distribution spans a dynamic range of ~ 100 to 1, it is difficult to completely eliminate an amplitude-dependent time shift. Amplitude selection would reduce the dynamic range, but it has not been established that the time distribution and the amplitude distribution are completely independent.

Preliminary work on time spreads shows the following ranges for gate widths

Tube type	Gate width to pass 90% of single-electron pulses (nsec)
1P21	1.3
6810-A	13
7819	84
9530-B	115

To obtain high counting efficiency at very low light levels, one must use sufficiently wide gates. The chance of an accidental noise pulse increases with gate width. The last column of Table I shows the number of noise counts per 10^4 gates if the gate width is set to pass 90% of the single-electron pulses and the discriminator is set at the plateau.

Conclusions

Measurements of the single-electron pulse-height distribution from an electron multiplier approximate a distribution calculated from Poisson statistics. Measurements by others have indicated an exponential distribution, but we believe that their result is due to the presence of noise.

Since the counting rate of photomultiplier and other noise rises rapidly as the discriminator threshold is lowered, whereas the signal counting rate tends to reach a plateau, it is possible to optimize the discriminator threshold for signal-to-noise pulse rate.

If the mean pulse gain of the multiplier is 10^6 or more, at least 90% of all the single-electron output pulses can be counted with negligible contributions from thermal and amplifier noise. The photomultiplier noise contribution will depend on the product of its noise rate and transit-time spread.

From Fig. 7 and 8 it is evident that large cathode-area photomultipliers have substantially lower collection efficiency than do the smaller tubes. Improved electron-optical design is necessary to solve the problem of focusing electrons from a large cathode into the first dynode without sacrificing timing accuracy.

The time necessary to collect data having small fluctuations can be reduced by employing a high repetition-rate light flasher.

Acknowledgment

We would like to express our appreciation to Mr. E. T. Clark and other members of the Nuclear Instrumentation Groups for their assistance, and especially to Mr. Cordon R. Kerns for supplying photomultiplier-gain, dark-current, and quantum-efficiency data.

References

1. Quentin A. Kerns, Frederick A. Kirsten, and Gerald C. Cox, Generator of Nanosecond Light Pulses for Phototube Testing, Rev. Sci. Instr. 30, 31 (1959).
2. Quentin A. Kerns, Frederick A. Kirsten, and Gerald C. Cox, A Generator of Fast-Rising Light Pulses for Phototube Testing, LRL Counting Handbook 3307, File No. CC8-30, January 1959.
3. Thomas A. Nunamaker, Arthur E. Bjerke, and Quentin A. Kerns, Pulse Shaping and Standardizing of Photomultiplier Signals for Optimum Timing Information Using Tunnel Diodes, Lawrence Radiation Laboratory Report UCRL-9838, August 30, 1961.
4. A. Van der Ziel, Noise, (Prentice Hall, Inc., New York, 1954) pp. 113-115.
5. J. A. Baicker, "Dark Current in Photomultipliers," in Proceedings of the Seventh Scintillation Counter Symposium, Washington D. C., February 25-26, 1960, I. R. E. Trans. Nucl. Sci. 7, 74 (1960).
6. Statistics of Electron Multiplication, F. J. Lombard and F. Martin, Rev. Sci. Instr. 32, 200 (1961).

Figure Legends

Fig. 1. Block diagram of system for measuring single-electron statistics.

Fig. 2. Low-level shielding details and charge-calibration circuit.

Fig. 3. Calculated amplitude distribution of pulses from an electron multiplier for single-electron inputs. A Poisson distribution of secondary emission and an equal average gain per stage, m, is assumed (from F. J. Lombard and F. Martin, Ref. 8.).

Fig. 4. Calculated single-electron counting rate as a function of discriminator threshold (obtained by integrating the curves of Fig. 3.) A discriminator level of 100 corresponds to the mean pulse amplitude (m is the average gain per stage).

Fig. 5. Measured amplitude distribution of anode pulses due to single-photoelectron inputs for a CL-1090 photomultiplier ($m \approx 3$). A curve of xe^{-x} is included for comparison.

Fig. 6. Experimental single-electron pulse counting rates for several photomultipliers. A discriminator level of approximately 1.0 corresponds to the mean of the pulse amplitude distribution.

Fig. 7. Relative single-electron pulse counting rate vs illuminated cathode area for 2-in. photomultipliers. An aperture is located between the photocathode and the low-intensity light pulser to adjust the illuminated cathode area.

Fig. 8. Relative single-electron pulse counting rate vs illuminated cathode area for 5-in. photomultipliers. An aperture is located between the photocathode and the low-intensity light pulser to adjust the illuminated cathode area.

Table I. Comparison of Measured Dark-Current Counting Rates[a] with Hypothetical Cathode Electron Emission Rates[b]

Photomultiplier Type	D C Gain	Measured Rate (kc/sec)	Calculated Rate (kc/sec)	Noise Counts per 10^4 Gates
Reflection-type cathode				
RCA 1P21	5×10^6	130	600	2
Two-inch transmission-type cathode				
DuMont 6292	1.3×10^6	3,000 330@ -35°C	9,000 -----	- 100
CBS CL-1090	1.0×10^7	3	6	0.5
RCA 6810-A	2.0×10^7	66	90	9
RCA 6655-A	2.5×10^6	330	-----	-
Five-inch transmission type cathode				
RCA 7046	3.0×10^7	60	60	9
CBS 7819	2.0×10^6	66	150	56
DuMont 6264	3.0×10^6	200	200	120
Radiotechnique 58AVP	3.0×10^7	160	250	11
EMI 9530-B	3.0×10^7	40	180	46

(a) The discriminator charge sensitivity has been set at the plateau for counting single photoelectrons. Ambient temperature was ~ 25°C except for the 6292 (as noted).

(b) A hypothetical electron-emission rate $N_{calc.}$ at the cathode is:

$$N_{calc.} = \frac{\text{Anode dark current (amps)}}{\text{DC gain} \times 1.602 \times 10^{-19} \text{ (coulombs)}}$$

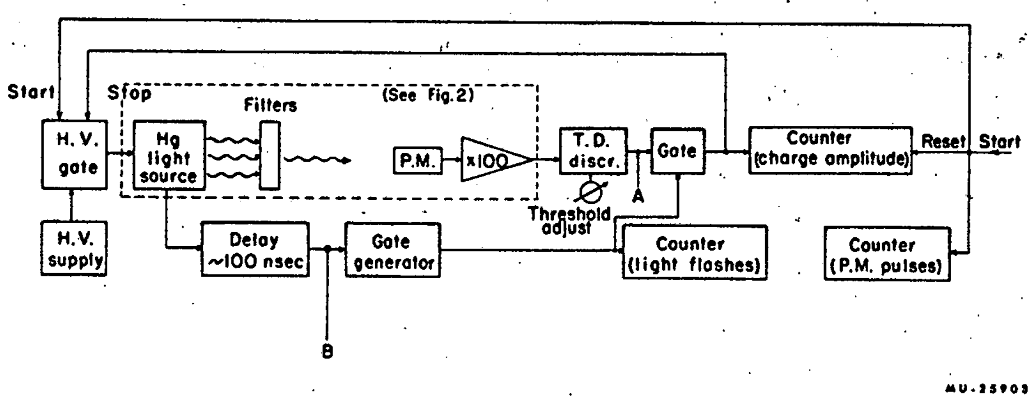
Start
Stop
(See Fig. 2)
Filters
H. V. gate
Hg light source
P.M.
x100
T. D. discr.
Gate
Counter (charge amplitude)
Reset
Start
Threshold adjust
A
H.V. supply
Delay ~100 nsec
Gate generator
Counter (light flashes)
Counter (P.M. pulses)
B
MU-25903

Fig. 1

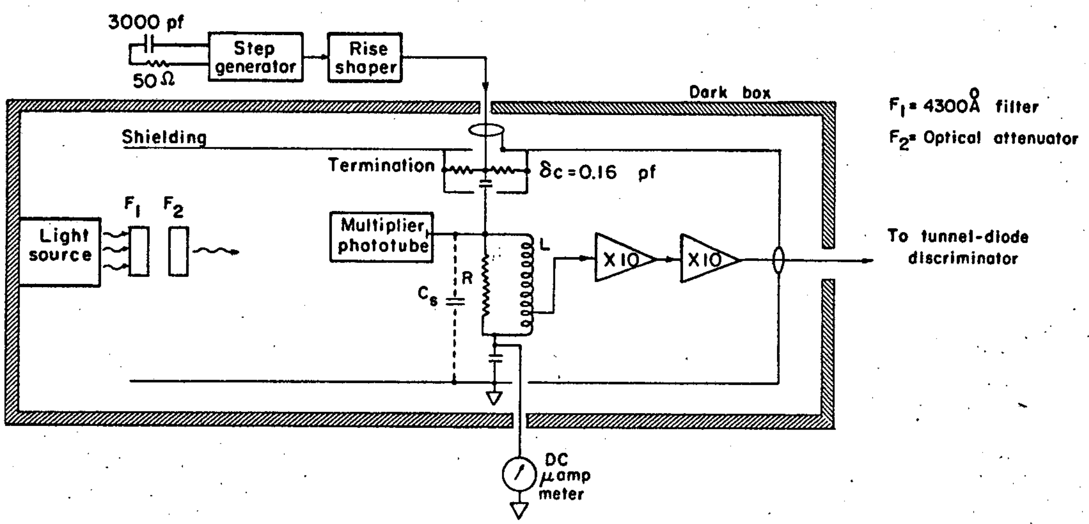
3000 pf
50 Ω
Step generator
Rise shaper
Dark box
Shielding
Termination
δc = 0.16 pf
Light source
F1
F2
Multiplier phototube
L
R
Cs
X10
X10
DC μamp meter
F1 = 4300Å filter
F2 = Optical attenuator
To tunnel-diode discriminator
MU-25904

Fig. 2

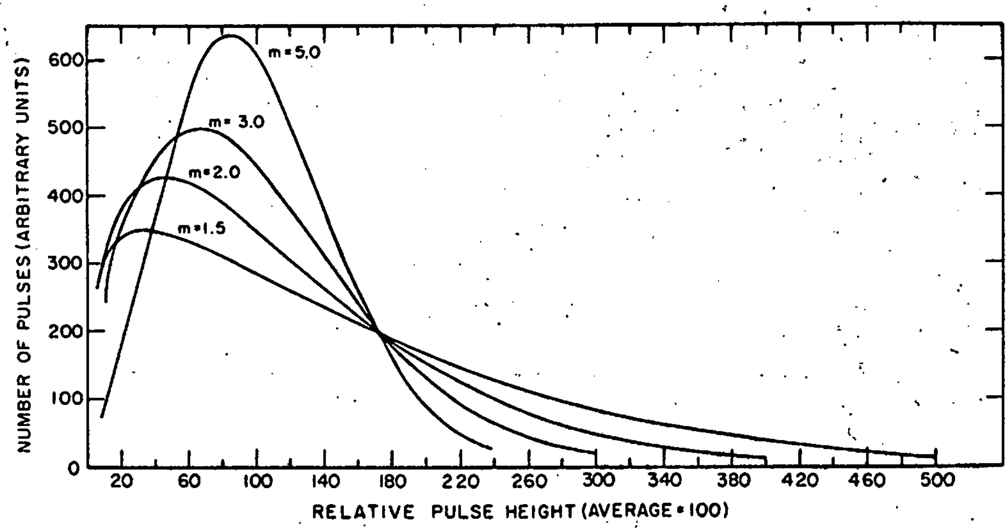

MU-25999

Fig. 3

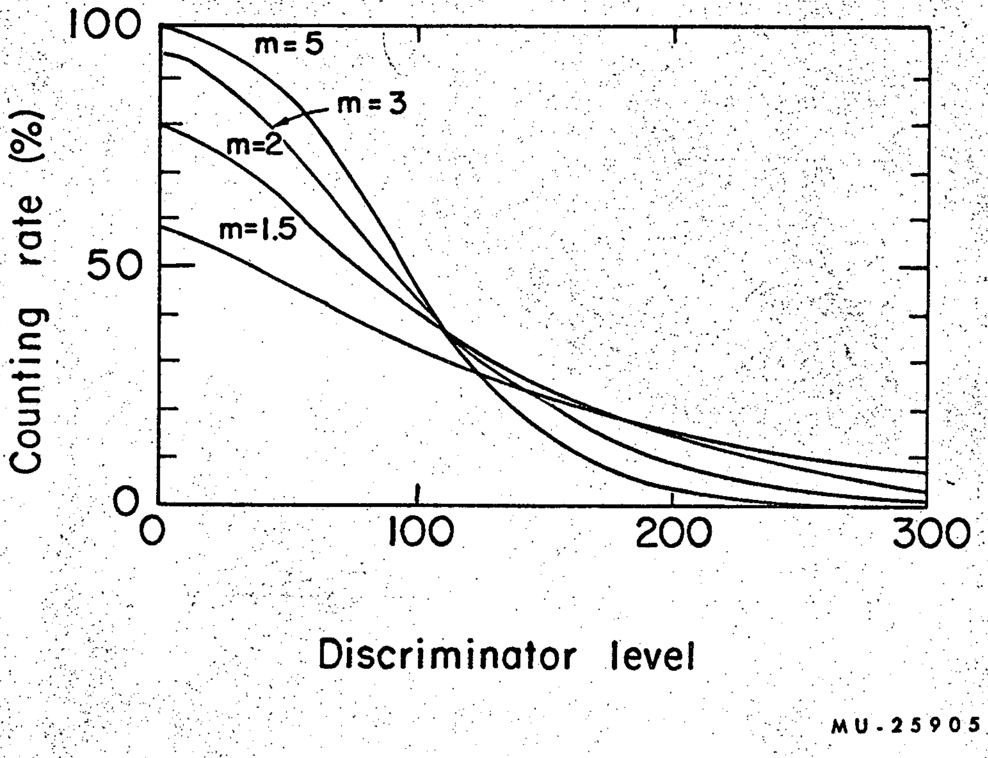

100
50
0
0
100
200
300
m=5
m=3
m=2
m=1.5
Counting rate (%)
Discriminator level
MU-25905

Fig. 4

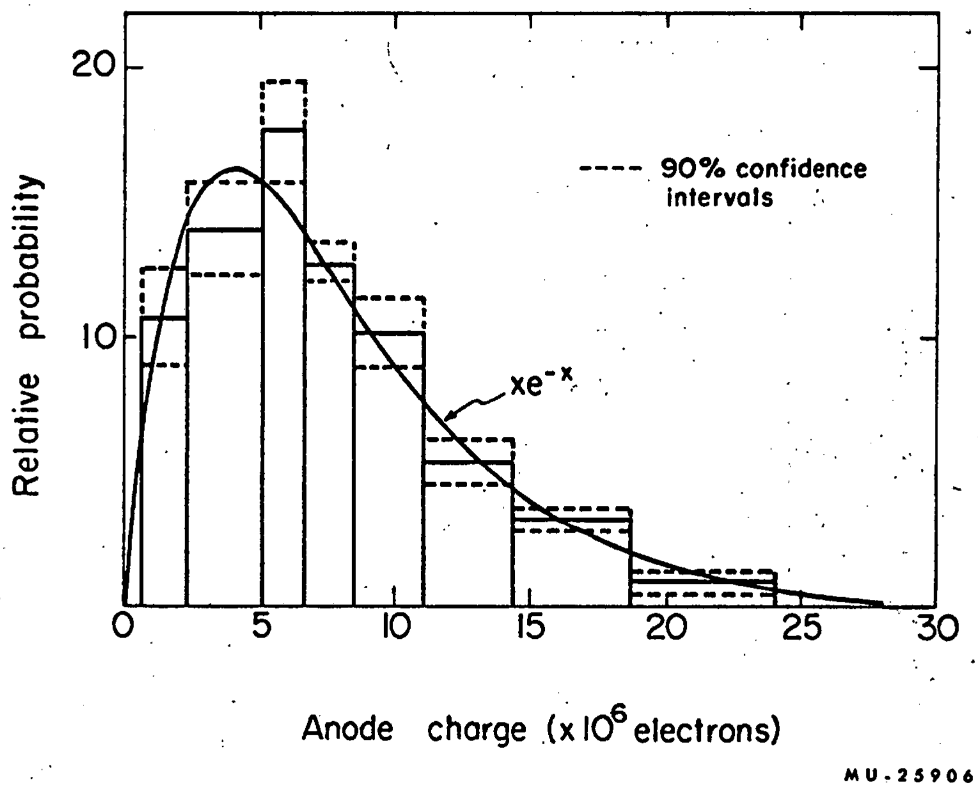
Relative probability
20
10
0
5
10
15
20
25
30
Anode charge (x 10⁶ electrons)
---- 90% confidence intervals
xe^-x
MU-25906

Fig. 5

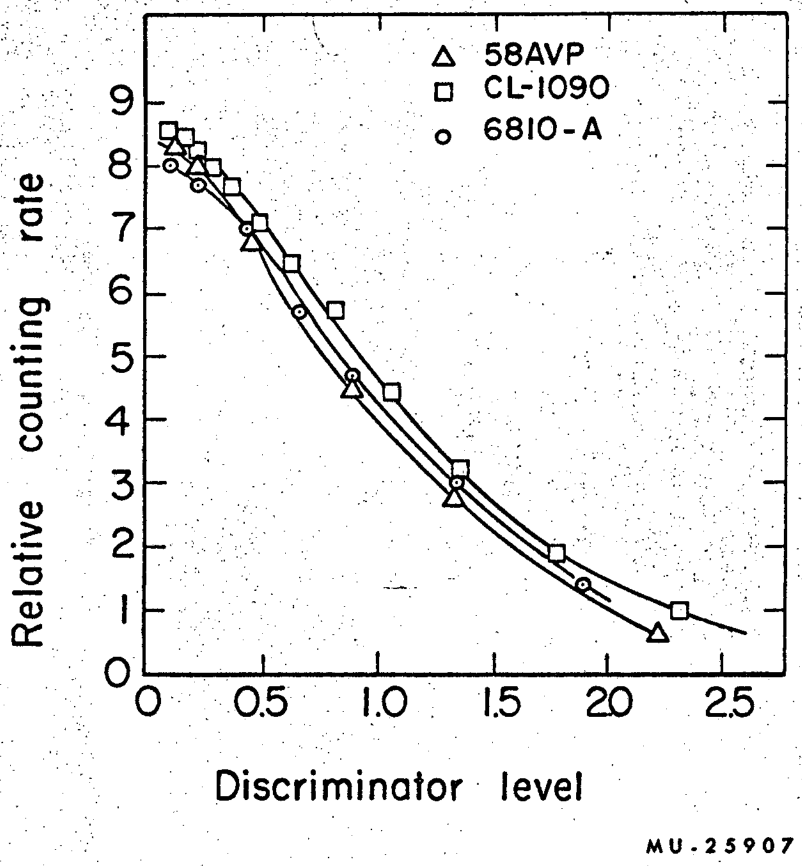
58AVP
CL-1090
6810-A
Relative counting rate
0
1
2
3
4
5
6
7
8
9
0
0.5
1.0
1.5
2.0
2.5
Discriminator level
MU-25907

Fig. 6

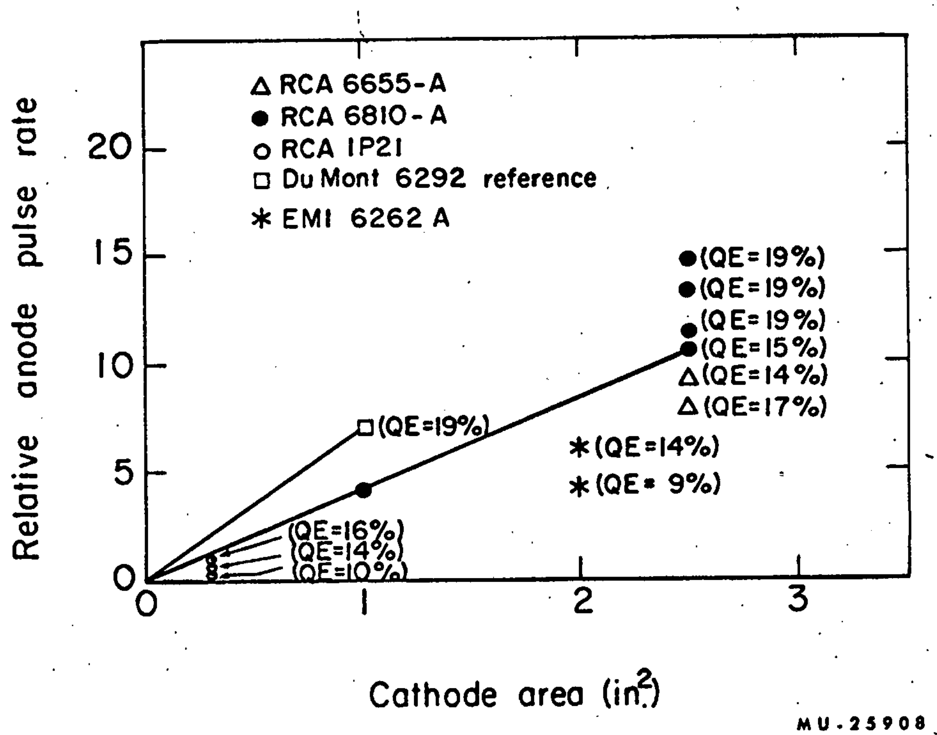

△ RCA 6655-A
● RCA 6810-A
○ RCA 1P21
□ Du Mont 6292 reference
* EMI 6262 A
●(QE=19%)
●(QE=19%)
●(QE=19%)
●(QE=15%)
△(QE=14%)
△(QE=17%)
□(QE=19%)
*(QE=14%)
*(QE= 9%)
(QE=16%)
(QE=14%)
(QE=10%)
Relative anode pulse rate
Cathode area (in.²)
0
5
10
15
20
1
2
3
MU-25908

Fig. 7

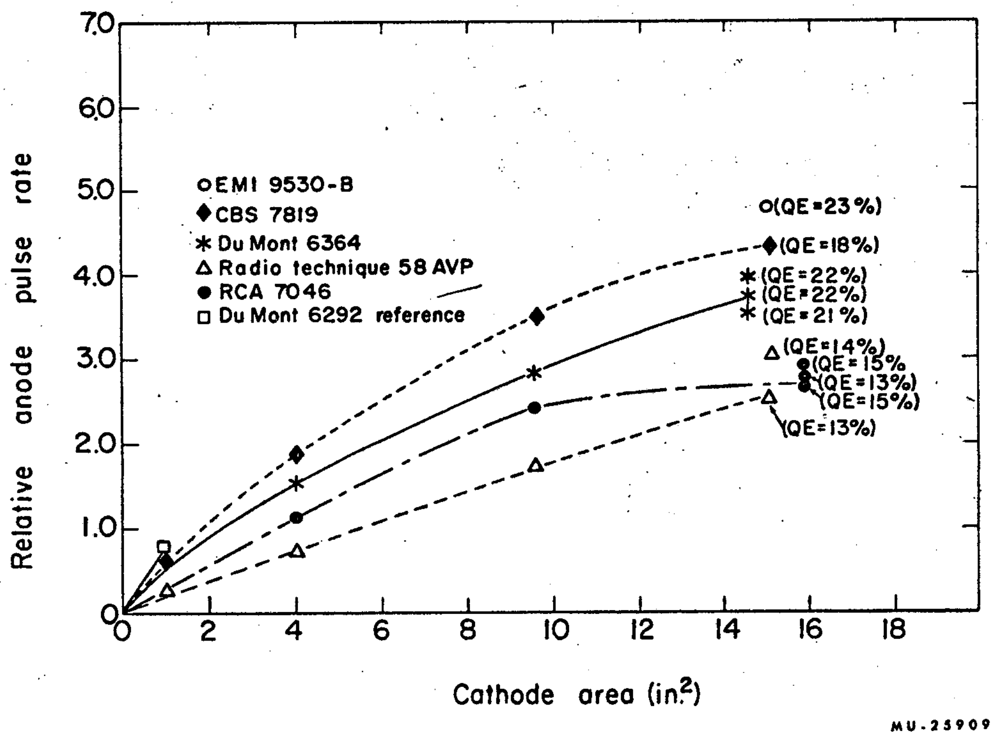

7.0
6.0
5.0
4.0
3.0
2.0
1.0
0
Relative anode pulse rate
EMI 9530-B
CBS 7819
Du Mont 6364
Radio technique 58 AVP
RCA 7046
Du Mont 6292 reference
(QE = 23 %)
(QE = 18%)
(QE = 22%)
(QE = 22%)
(QE = 21 %)
(QE = 14%)
(QE = 15%)
(QE = 13%)
(QE = 15%)
(QE = 13%)
0
2
4
6
8
10
12
14
16
18
Cathode area (in.^{2})
MU-25909

Fig. 8